McKenzie D. and J. Jackson; 2002: Conditions for flow in the continental crust, *Tectonics*, 21, doi:10.1029/2002TC001394.

McKenzie D. P.; 1977: The initiation of trenches: a finite amplitude instability, in *Island Arcs, Deep Sea Trenches, and Back-Arc Basins*, vol. 1, edited by M. Talwni and W. C. P. III, pp. 57-61, Am, Geophysics. Un., Washington, D. C., Maurice Ewing Ser.

Mueller S. and R. J. Phillips; 1991: On the initiation of subduction, *J. Geophys. Res.*, 96 (B1), 651-665.

SLIP DISTRIBUTION FOR THE 2004 SUMATRA-ANDAMAN EARTHQUAKE CONSTRAINED BY BOTH GPS DATA AND TSUNAMI RUN-UP MEASUREMENTS

K.L.H. Hughes, T. Masterlark

Department of Geological Sciences, The University of Alabama, Tuscaloosa, AL 35487 (USA)

Summary

The M9.3 Sumatra-Andaman earthquake (SAE) of 26 December 2004 ruptured over 1200 km of crust separating the subducting Indo-Australian plate and overriding Burma microplate. Various geodynamic models have been created to quantitatively examine the SAE. To date, no investigators have modeled onshore near-field coseismic deformation and seafloor deformation required by tsunami run-up measurements simultaneously. We identify the inconsistency between various slip distributions and provide an alternative that satisfies both onshore and offshore deformation requirements. Our results suggest (1) A forward model driven by slip distribution derived from tsunami run-ups fails to adequately predict observed near-field GPS data, although it adequately matches far-field observed GPS data, (2) GPS-based slip distribution estimations, that allow for dip-slip only, either poorly predicts near-field observed GPS data or are prohibitively rough, and (3) More complex models that allow for both strike-slip and dip-slip dislocations are needed to adequately simulate both onshore and offshore near-field deformation.

Introduction

Over 1200 km of the Sumatra-Andaman subduction zone (SASZ) was ruptured during the 26 December 2004 M9.3 Sumatra-Andaman earthquake (SAE) (Bilek, 2007; Sørensen et al., 2007). This event induced a devastating tsunami that killed over 250,000 people in over 12 countries (Rastogi and Jaiswal, 2006). The SASZ is a large subduction zone in which the Indo-Australian Plate subducts beneath the Sunda Plate and Burma microplate (Fig. 1). The SAE is the largest earthquake recorded by GPS, and presents a unique opportunity to quantify the coseismic deformation. An accurate description of the fault-slip distribution for the SAE is key to any analysis of coseismic deformation, postseismic deformation, postseismic stress-coupling, and tsunami-genesis. The fault-slip of the SAE deformed the overlying seafloor, with a vertical deformation pattern that served as initial conditions for tsunami genesis models (e.g., Grilli et al., 2007). An accurate coseismic slip distribution is a prerequisite for quantitative interpretations of coseismic deformation.

Several coseismic slip distributions have been published for the SAE, based on either the near-field or far-field GPS data or both data sets (Catherine et al., 2005; Banerjee et al., 2005; Gahalaut et al., 2006; Banerjee et al., 2007). All of these slip distributions adequately fit the far-field GPS data. Alternatively, tsunami run-up measurements were recorded on many coastlines surrounding the Indian Ocean. These data can also be used to quantify the coseismic seafloor deformation and thus, the slip distribution for the SAE. Several different slip distributions have been estimated based on tsunami run-up measurements (Chlieh et al., 2007; Fujii and Satake, 2007; Piatanesi and Lorito, 2007; Grilli et al., 2007). The SAE caused a continuous coseismic deformation field, which can be measured by GPS at onshore locations. The offshore portions of the deformation field induced instabilities in the overlying water column, for which the subsequent propagation lead to tsunami run-up measurements. Unfortunately, previously reported slip distributions estimated from either GPS or tsunami run-up measurements have been incompatible. Comparing any slip distribution solely based on GPS to any slip distribution solely based on tsunami run-up measurements reveals that neither slip distribution matches the other adequately. Both

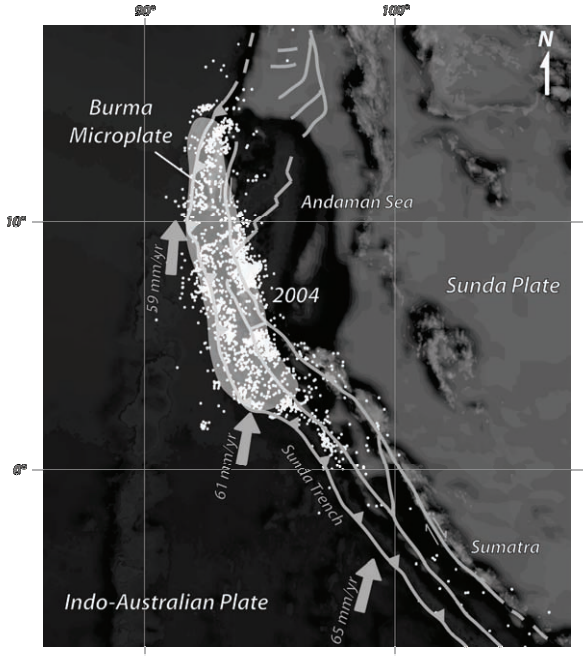

Figure 1. Seismotectonic setting of the SASZ. White circles represent aftershocks between 26 December 2004 and 28 March 2005. Light gray translucent area shows projection of rupture at the land surface.

onshore and offshore deformation was generated by the SAE. A common slip distribution should satisfy both GPS and tsunami run-up data.

We propose that a more complex slip distribution is required to simultaneously account for both near-field GPS data and seafloor deformation required by tsunami run-up measurements. We examine the differences in GPS deformation predicted by forward models of slip distributions estimated from tsunami run-up measurements (e.g., Grilli et al., 2007) and differences in a corresponding slip distribution estimated from inverse models of GPS data. We then compare these homogeneous, elastic, half-space (HEHS) models to more complex heterogeneous finite element models (FEMs) to determine which model best predicts both the tsunami run-ups and GPS data.

Methods

Models of deformation due to a dislocation embedded in an HEHS are readily available (Okada, 1992). HEHS models, and to a lesser extent layered elastic half-space models (LEHS), are commonly implemented to estimate slip distributions from tsunami run-up measurements and far-field and near-field GPS data (Chlieh et al., 2007; Banerjee et al., 2007; Gahalaut et al., 2006). However, these data have not been used to derive a single slip distribution that simultaneously honors both onshore and offshore deformation requirements of GPS and tsunami run-up measurements.

We use a slip distribution having five fault patches, following the configuration proposed by Grilli et al. (2007) that is based on tsunami run-up measurements, to predict deformation observed at 39 near-field and far-field GPS locations (Subarya et al., 2006; Gahalaut et al., 2006). The forward model for this linear system is

$$\boldsymbol{Gm} = \boldsymbol{d} \qquad (1)$$

where $\boldsymbol{G}$ is a matrix of Green's functions for deformation due to a dislocation, $\boldsymbol{m}$ is a vector that corresponds to a slip distribution, and $\boldsymbol{d}$ is a vector of displacement data (Menke, 1989). The data vector is constructed from all three GPS displacement components. Sensitivities of deformation to a given slip distribution can be estimated by comparing forward model predictions to observed GPS data.

In addition to comparing GPS vectors, we construct inverse models to estimate the slip distribution for the five fault patches, based on near-field GPS data. The least-squares solution for the slip distribution is

$$\boldsymbol{m}^{est} = [(\boldsymbol{WG})^{T}(\boldsymbol{WG})]^{-1}(\boldsymbol{WG})^{T}(\boldsymbol{Wd}) \quad (2)$$

where $\boldsymbol{m}^{est}$ is the estimated slip distribution and $\boldsymbol{W}$ is a weighting matrix constructed from GPS measurement uncertainties (Menke, 1989). The optimal slip inversion had four reverse (thrust) fault patches and one normal fault patch. Because normal slip is not a geologically reasonable result, we invoked smoothing constraints using a Laplacian operator,

$$\begin{bmatrix} \boldsymbol{WG} \\ \beta\boldsymbol{L} \end{bmatrix}[\boldsymbol{m}] = \begin{bmatrix} \boldsymbol{Wd} \\ 0 \end{bmatrix} \quad (3)$$

where $\boldsymbol{L}$ is a Laplacian smoothing matrix, a null vector appends the weighted data matrix, and β is a damping parameter that controls the tradeoff of misfit versus solution complexity (Menke, 1989). All five fault patches of the resulting slip distribution are positive (thrust) and can be compared to the corresponding slip distribution estimated from tsunami run-ups.

We construct FEMs to explore sensitivities of forward and inverse model predictions to problem domain complexities beyond the restrictions of HEHS and LEHS models. We compute FEM-generated Green's Functions (Masterlark, 2003) for displacement due to a dislocation in a 3-D heterogeneous problem domain (Fig. 2). Although computationally expensive, FEMs allow us to honor the known geologic complexity of the SASZ. In particular, neither HEHS nor LEHS models can account for the presence of the relatively stiff subductiong plate. The plate is the first order feature of a subduction zone and significantly impacts both forward and inverse models of coseismic deformation (Masterlark, 2003).

Results

We forward modeled the five fault patch tsunami slip distribution for dip-slip only (Grilli et al., 2007) to determine the predicted data vectors for 39 GPS station locations. The resulting vectors poorly predict the observed GPS data (Fig. 3a). We inverse modeled both the near-field and far-field GPS data for the five fault patches with dip-slip only. The estimated dip-slip distribution adequately matches the far-field GPS data (Fig. 3b), but does not match the near-field GPS data (Fig. 3c).

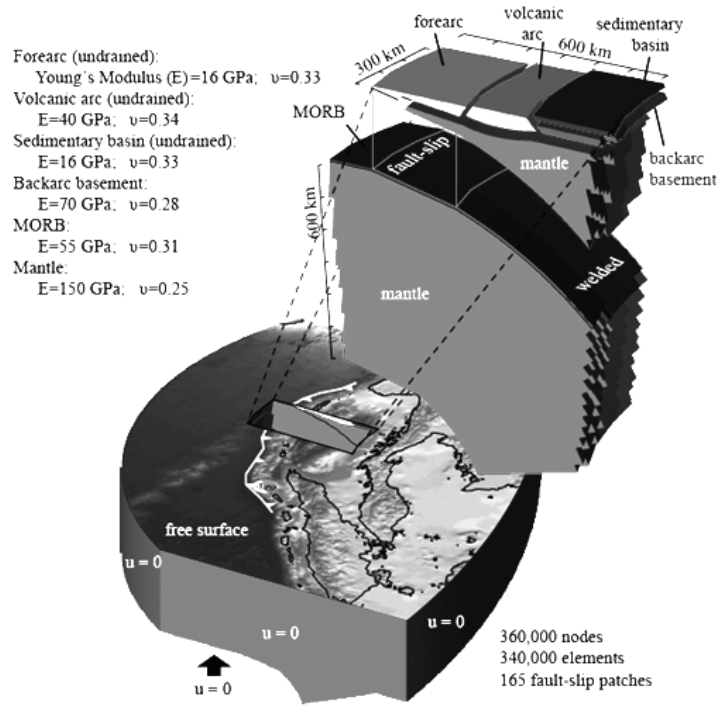

Figure 2. FEM problem domain. Inset shows exploded cross-section view. Cross-section was propagated along strike to create 3-D FEM.

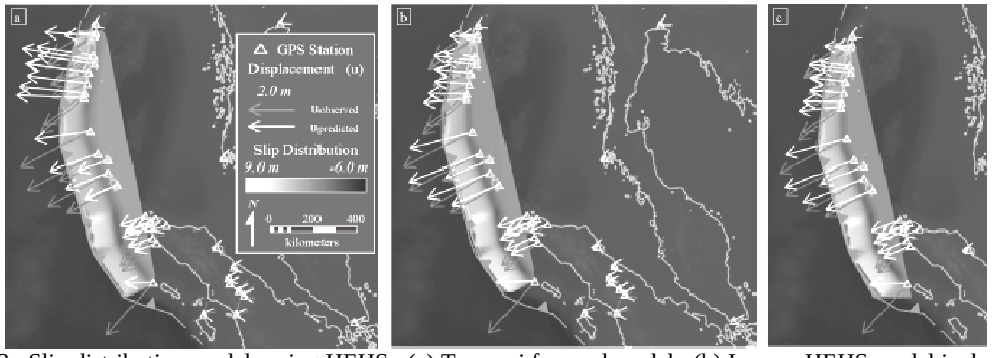

Figure 3. Slip distribution models using HEHS. (a) Tsunami forward model. (b) Inverse HEHS model including all 38 GPS stations. (c) Inverse HEHS model including 28 near-field GPS stations. Slip distributions are shown in grayscale contours. Negative anomalies surrounded by positive deformation are an artifact of coarse grid spacing. Gray arrows represent observed GPS, and white arrows represent predicted GPS.

We inverse modeled the GPS data using an FEM to simulate a more refined slip distribution along the curved surface of the rupture. Increasing the number of fault patches and accounting for varying rock properties, adequately predicts the observed GPS data based on a dip-slip only distribution (Fig. 4a). However, the desirable misfit comes at the expense of a very rough slip distribution. Another inverse model constructed with FEM-generated Green's Functions allows for both strike-slip and dip-slip dislocations. This latter FEM appears to better match the near-field GPS data, but still does not put large slip near the trench where it is needed for accurate tsunami models (Fig. 4b) (Grilli et al., 2007). A third inverse FEM allows for both dip-slip and strike-slip dislocations and includes constraints that favor shallow slip in an effort to satisfy both onshore deformation required by the GPS data and seafloor deformation required by tsunami run-up measurements (Grilli et al., 2007).

Discussion

The deformation predictions from the slip distribution estimated from tsunami run-ups adequately predict the far-field GPS deformation, but poorly predict near-field GPS deformation (Fig. 3). This suggests that the complex deformation nearest the rupture must be resolved for quantitative tsunami-genesis analyses, in accord with seismological observations (Engdahl et al., 2007). Furthermore, the geology of the SASZ is readily accounted for by incorporating varying material properties in the FEM. These material properties significantly influence the individual elements of the $\boldsymbol{G}$ matrix and thus strongly affect estimations of slip distribution (Masterlark, 2003). Comprehensive sensitivity analyses of material properties, problem domain configurations, and associated slip-distribution estimation methods will be addressed in future analyses.

We can fit GPS data with our FEM using a distribution of dip-slip dislocations alone, but the distribution is excessively rough (Fig. 4). Alternatively, a smoother distribution poorly predicts the near-field GPS data. However, allowing for strike-slip dislocations, in addition to dip-slip dislocations, appears to provide reasonable misfit, as well as a relatively smooth slip distribution. Furthermore, additional constraints on the shallow slip result in a slip distribution having desirable misfit and smoothness, produce seafloor deformation that is consistent with tsunami-run-up measurements. Our slip distribution is consistent with that produced by using a splay fault to create large seafloor deformation (Hoechner et al., 2008).

The SASZ is an obliquely converging tectonic setting. Near the Andaman Islands the plate motions are accommodated almost completely by strike-slip motion. Aftershock activity between the M9.3 SAE and the M8.7 Nias earthquake shows a significant increase in strike-slip motion and normal faulting at the northern end of the rupture (Engdahl et al., 2007). Our results match seismicity data, suggesting that dip-slip only is not an adequate assumption for resolving GPS data in the Andaman Islands.

Our results illustrate that near-field GPS data dominate the inverse slip distribution and far-field GPS data are well fit using a five fault patch dip-slip only HEHS model (Fig. 3). Both forward deformation predictions and estimated slip distributions are strongly model dependent, a result that suggests model

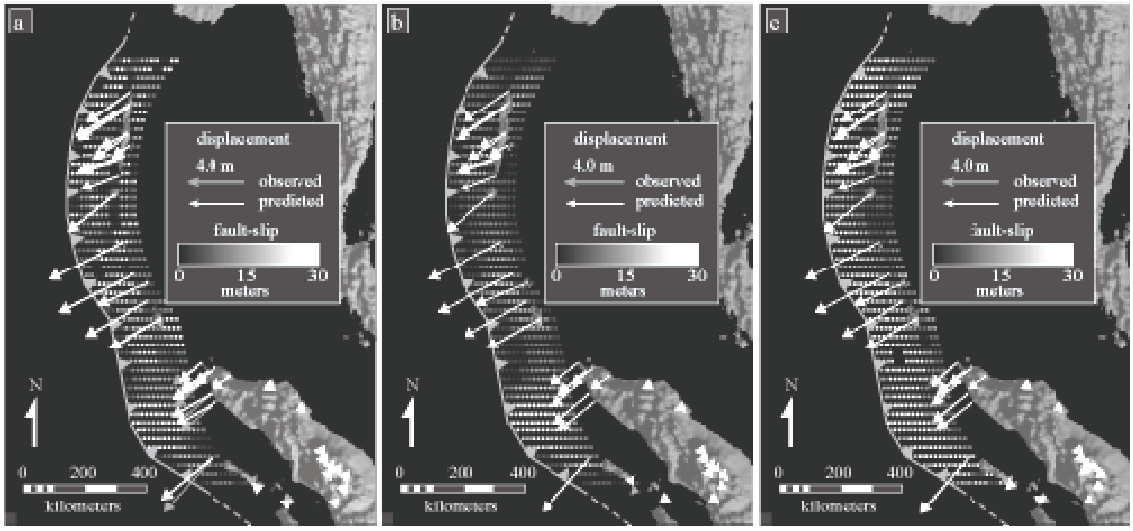

Figure 4. Slip distribution models using FEMs. (a) FEM inverse model for dip-slip only. (b) FEM inverse model for dip-slip and strike-slip. (c) FEM inverse model for dip-slip, strike-slip and increased shallow slip near the accretionary wedge. Slip distribution is shown by grayscale dots. Gray arrows represent observed GPS, and white arrows represent predicted GPS.

design is critical to quantitative analyses of coseismic deformation and associated processes, such as tsunami-genesis, stress-coupling, and postseismic deformation.

Conclusions

We tested the hypothesis that an estimated slip distribution can predict observed GPS data and seafloor deformation required for tsunami run-up measurements simultaneously. We determined that onshore deformation predicted for a slip distribution, estimated based on tsunami run-up measurements (Grilli et al., 2007), does not match the observed near-field GPS data (Subarya et al., 2006; Gahalaut et al., 2006), but adequately predicts far-field GPS data. A more complex model configuration, allowing for both dip-slip and strike-slip dislocations, is required to adequately simulate the observed onshore near-field deformation while simultaneously producing elevated magnitudes of seafloor deformation required for tsunami run-up observations.

Acknowledgments

Support provided by NASA NIP (NNX060F10G). Academic licensing for Abaqus software was provided by Simulia Inc.

REFERENCES

Banerjee P., Pollitz F. F. and Bürgmann R.; 2005: *The size and duration of the Sumatra-Andaman earthquake from far-field static offsets*. Sci., 308, 1769-1772.

Banerjee P., Pollitz F., Nagarajan B. and Bürgmann R.; 2007: *Coseismic slip distributions of the 26 December 2004 Sumatra-Andaman and 28 March 2005 Nias earthquakes from GPS static offsets*. Bull. Seis. Soc. Am., 97, S86-S102.

Bilek S. L.; 2007: *Using earthquake source durations along the Sumatra-Andaman subduction system to examine fault-zone variations*. Bull. Seis. Soc. Am., 97, S62-S70.

Catherine J. K., Gahalaut V. K. and Sahu V. K.; 2005: *Constraints on rupture of the December 26, 2004, Sumatra earthquake from far-field GPS observations*. Ear. Pla. Sci. Let., 237, 673-679.

Chlieh M., Avouac J.-P., Hjorleifsdottir V., Song T.-R. A., Ji C., Sieh K., Sladen A., Hebert H., Prawirodirdjo L., Bock Y. and Galetzka J.; 2007: *Coseismic slip and afterslip of the great* M_w *9.15 Sumatra-Andaman earthquake of 2004*. Bull. Seis. Soc. Am., 97, S152-S173.

Engdahl E. R., Villaseñor A., DeShon H. R. and Thurber C. H.; 2007: *Teleseismic relocation and assessment of seismicity (1918-2005) in the region of the 2004 M_w 9.0 Sumatra-Andaman and 2005 M_w 8.6 Nias Island great earthquakes*. Bull. Seis. Soc. Am., 97, S43-S61.

Fujii Y. and Satake K.; 2007: *Tsunami source of the 2004 Sumatra-Andaman earthquake inferred from tide gauge and satellite data*. Bull. Seis. Soc. Am., 97, S192-S207.

Gahalaut V. K., Nagarajan B., Catherine J. K. and Kumar S.; 2006: *Constraints on 2004 Sumatra-Andaman earthquake rupture from GPS measurements in Andaman-Nicobar Islands*. Ear. Pla. Sci. Let., 242, 365-374.

Grilli S.T., M.ASCE, Ioualalen M., Asavanant J., Shi F., Kirby J. T., M.ASCE and Watts P.; 2007: *Source constraints and model simulation of the December 26, 2004, Indian Ocean tsunami*. Jrl. Wat., Port, Cst., Oc. Eng., 133, 414-428.

Hoechner A., Babeyko A. Y. and Sobolev S. V.; 2008: *Enhanced GPS inversion technique applied to the 2004 Sumatra earthquake and tsunami*. Geo. Res. Let., 35.

Masterlark T.; 2003: *Finite element model predictions of static deformation from dislocation sources in a subduction zone: Sensitivities to homogeneous, isotropic, Poisson-solid, and half-space assumptions*. Jrl. Geo. Res., 108.

Menke W.; 1989: *Geophysical Data Analysis: Discrete Inverse Theory*. Academic Press Inc., San Diego.

Okada Y.; 1992: *Internal deformation due to shear and tensile faults in a half-space*. Bull. Seis. Soc. Am., 82, 1018-1040.

Piatanesi A. and Lorito S.; 2007: *Rupture process of the 2004 Sumatra-Andaman earthquake from tsunami waveform inversion*. Bull. Seis. Soc. Am., 97, S223-S231.

Rastogi B. K. and Jaiswal R. K.; 2006: *A catalog of tsunamis in the Indian Ocean*. Sci. Tsu. Haz., 25, 128-143.

Sørensen, M. B., Atakan K. and Pulido N.; 2007: *Simulated strong ground motions for the great* M*9.3 Sumatra-Andaman earthquake of 26 December 2004*. Bull. Seis. Soc. Am., 97, S139-S151.

Subarya C. M., Chlieh M., Prawirodirdjo L., Avouac J.-P., Bock Y., Sieh K., Meltzner A. J., Natawidjaja D. H. and McCaffrey R.; 2006: *Plate-boundary deformation associated with the great Sumatra-Andaman earthquake*. Nat., 440, 46-51.

EPISODIC SLAB ROLLBACK MAKES IT EASY FOR HIGH PRESSURE ROCKS TO REACH THE SURFACE

L. L. Husson[(1)], J-P. Brun[(1)], C. Faccenna[(2)], F. Gueydan[(1)]

[(1)] *Géosciences Rennes, CNRS, Université Rennes-1 (France)*
[(2)] *Dipartimento di Scienze Geologiche, Univ. Roma-3 (Italy)*

Summary
The transient subduction of units of variable buoyancies along a slab is associated to an episodic subduction regime. In particular, slab geometry and trench migration respond very efficiently to the buoyancy variations of the slab. For instance, the subduction of a continental unit embedded within an oceanic slab that has a negative buoyancy is accompanied by a slowdown in migration rates and increase of the slab dip, which is followed by an episode of increase in trench migration rates and decrease in slab dip, during which exhumation occurs. We compute the associated flow in the subduction wedge for three distinct situations: (i) stationary subduction, which is not prone to the exhumation of HP rocks, (ii) slab rollback at constant dip that is more favorable, and (iii) slab rollback accompanied by a decrease in slab dip, in which case the upward flow in the wedge is extremely efficient and invariably causes the exhumation of rock units a depth. The latter situation corresponds to transient episodes of slab rollback.

Introduction
The mechanism for exhumation of high pressure metamorphic rocks in Phanerozoic belts has been debated for long and a variety of models have been proposed (e.g. Cloos, 1982; Mancktelow, 1984, Chemenda et al., 1995, Gerya et al., 2002; Yamato et al., 2007). Subducting slabs can easily convey rocks at large depths before they detached from the slab and gradually find their route to the surface. Contrarily, deciphering the mechanism for exhumation is much more challenging and the many hypothesis made so far are difficult to reconcile with observations. Models commonly involve channel-flow (e.g. Cloos et al., 1982; Gerya et al.,2002), delamination (Chemenda et al., 1995) or slab break-off (Ernst et al., 1997).